Research Article

Parametric investigation of surface texturing on performance characteristics of water lubricated journal bearing using FSI approach

Anil B. Shinde[1] · **S. P. Chavan**[1]

Received: 6 September 2019 / Accepted: 27 November 2019 / Published online: 6 December 2019

Abstract
In this paper, parametric analysis of various operating and surface texturing parameters on the performance characteristics of water lubricated journal bearing was carried out using Fluid Structure Interaction approach. Initially, a simulation model was validated with experimental results from the literature. An effect of journal speed and eccentricity ratio along with elastic deformation on performance characteristics viz. lubricant pressure, load carrying capacity, and coefficient of friction with different groove location was studied. Further investigation was carried out to examine the influence of the number of grooves on the performance characteristics. From the analysis, it was observed that 0–180° grooved journal bearing with 5 number of grooves has shown improved performance as compared to journal bearing with 0–90° grooved, 90–180° grooved and plain surface.

Keywords Fluid Structure Interaction · Water lubricant · Surface texturing · Fluid film pressure · Coefficient of friction · Load carrying capacity

1 Introduction

Working of machines with high efficiency, more energy saving and decreasing the environmental pollution is become important criteria in machine design [1]. Hydrodynamic journal bearings are broadly used in applications such as electric generators, gas turbines, hydro turbines, IC Engines, marine propellers, turbo generators and hard disk drives due to their simplicity and superior damping characteristics [2]. Use of water as lubricant is become popular because of its safe, green, energy saving tendency and convenience. Because of this, water lubricated journal bearings are used in industrial machinery, shipbuilding, food industry, transportation industry and pharmaceutical industry [3]. Wang et al. [4] studied load carrying capacity and friction using sliding surfaces of the polymer in water. They used Polytetrafluoroethylene (PTFE) material for bearing with the benefit of very small friction coefficient and good corrosion-resistant property, excellent chemical stability and water absorption. They concluded that for the lubrication performance of water-lubricated bearing, the deformation effect cannot be ignored. Su et al. [5] studied deformation of textured (dimple) surface in the soft elastohydrodynamic lubrication (EHL) contacts and showed that an uneven deformation emerges around a dimple. They also concluded that the sliding velocity and applied load have noteworthy influence on the deformation of soft surface, particularly on deformation area. Habchi et al. [6] carried out an investigation on the elastohydrodynamic line or point contact lubrication problem by pairing Reynolds equation and elastic deformation using a full-system approach. Gertzoset al. [7] investigated the performance characteristics of the journal bearing lubricated with the Bingham fluid using Computational Fluid Dynamic approach. The cavitation phenomenon is studies by implementing half-Sommerfeld boundary condition.

✉ Anil B. Shinde, anil.04.shinde@gmail.com | [1]Department of Mechanical Engineering, Annasaheb Dange College of Engineering & Technology, Ashta, Sangli, India.

Hartinger et al. [8] obtained a solution for thermal and shear thinning elastohydrodynamic line contact problem by employing a homogenous equilibrium cavitation model. Shenoy et al. [9] analysed an elastohydrodynamic lubrication of a hydrodynamic journal bearing employing the sequential application of CFD and computational structural dynamics and the cavitation was modeled by keeping all the calculated negative pressure and their gradients as zero. Liu et al. [10] investigated pressure distribution, cavitation and center orbit of journal of the elastohydrodynamic lubrication problem by employing using CFD and FSI methods. The bearing model in considered in their study was simple cylindrical journal bearing without any groove and thermal effects were not taken in account. Shinde et al. [11–15] studied an effect of partial groove shape texturing on performance characteristics of cylindrical shape journal bearing without considering the elastic deformation phenomenon. The performance characteristics were considered viz. fluid pressure, frictional torque, load carrying capacity (LCC) and power loss and concluded that groove shape texturing present in the positive pressure region enhances the performance of journal bearing. Further study extended for conical shape journal bearing along with ellipsoidal shape dimples texturing on bearing surface and enhanced the performance of bearing system. Shi et al. [16] investigated the influence of microdimples and microgrooves on the load-carrying performance of mechanical gas seals. They proved that both microgrooves and microdimples improve the load-carrying performance under a small clearance condition. Bouyer and Fillon [17] analyzed a single-groove plain journal bearing with thermoelastohydrodynamic (TEHD) effect under steady load in which elastic deformation of bearing surface and expansion of the journal were considered. Lin e al. [18] investigated the effect of surface texturing on the performance characteristics of hydrodynamic bearing working under the time dependant condition using fluid–structure interaction (FSI) method. In their analysis, displacements of journal and eccentricity ratio were considered as main parameters for actual operation of journal bearing. They showed that, location of texturing can increase or decrease the performance of a hydrodynamic bearing in terms of the developing the LCC. Profito and Zachariadis [19] implemented three partitioned fluid structure coupling methods to evaluate performance characteristics of steady state hydrodynamic journal bearings working in the elastohydrodynamic lubrication zone. Molka et al. [20] analyzed the influence of the bearing surface deformation on the performance of a cylindrical shape journal bearing. They employed the FEM with an iteration method for solving both the Reynolds equation and the three-dimensional elasticity expressions representing the displacement area in the bearing domain. They showed that elastic deformations extend the pressure area in the bearing and increase the minimum film thickness which reduces the LCC. Meng et al. [21] studied the effect of the compound dimple on the performance behavior of a journal bearing using a fluid structure interaction (FSI) method. They showed that the compound dimple can supply the larger load-carrying capacity and lower friction coefficient due to its twice hydrodynamic action in comparison with the simple dimple. Tala-Ighil et al. [22] examined the full and partial textured journal bearing for different working conditions. They concluded that, appropriate texture distribution iproves the film thickness, frictional torque and fluid pressure. Jadhav et al. [23] studied the influence of microtexturing on the performance of hydrodynamic bearing considering the elastic deformation behavior of bearing surface. They observed 38.28% reduction in coefficient of friction in textured bearing system. Tauviqirrahmam et al. [24] investigated the effect of surface texturing and slippage on the friction coefficient and load carrying capacity without considering the effect surface deformation of bearing. They showed 50% improvement in the load carrying capacity in case of textured bearing as compared to smooth surface bearing system. Tala-Ighil et al. [25] conducted numerical analysis of spherical shape dimple texturing on bearing surface and improved the performance of hydrodynamic bearing. They suggested that film thickness, fluid pressure, frictional torque and oil flow can be improved by introducing texturing in positive pressure zone. Gu et al. [26] suggested that, well designed texturing can reduce friction and positive influence on bearing performance. Cupillard et al. [27] studied the influence of texturing on load carrying capacity and friction.They showed that, texture of suitable geometry can reduce friction and increase load carrying capacity. Yu et al. [28] suggested that texturing introduced in rising phase of fluid pressure increases the load carrying capacity and reduces it in falling phase.

Hydrodynamic lubrication difficulties are mainly solved using the modified or classical Reynolds equation, which is derived from the fundamental Navier–Stokes equations. Although numbers of important CFD and experimental based investigations have been reported in which the effect of surface texture on the performance of oil lubricated journal bearings were studied without considering the effect of deformation of bearing surface. In all the studied investigations, either the bearing was treated as rigid or the lubricant was oil. It is very important to consider the effect of fluid pressure on the solid domain which significantly affects the performance behavior of bearing systems and there are very less reports about analysis of water lubricant based journal bearings with surface texturing using fluid–structure interaction approach.

Therefore, in this research, fluid structure interaction-based investigation of water lubricated surface textured journal bearing for various performance characteristics was carried out. The investigation of performance characteristics like development of fluid pressure, LCC, coefficient of friction and elastic deformation was performed at various operating and texturing conditions viz. speed of journal, eccentricity ratio and number of grooves. In this study, fluid structure interaction was implemented in which the effect of lubricant pressure on bearing surface was considered where journal domain was considered as rigid domain. The interest of work was consideration of bearing surface deformation due to fluid pressure and study the behavior of water lubricated surface textured journal bearings. This FSI approach provides realistic operating conditions of journal bearing along with surface texturing.

2 Fluid structure interaction (FSI) approach

In hydrodynamic journal bearing system, as journal rotates a continuous film of lubricant was developed between rotating journal and stationary bearing. The hydrodynamic positive pressure develop in lubricant in convergent region while terminates in divergent region. The pressure developed in lubricant film supports the external applied load. The FSI approach considers the actual operating condition of e journal bearing system. In this approach one way coupling between lubricant and bearing domain was examined. The governing equations used for this approach was described in this section.

2.1 Lubricant domain

The pressure in lubricant was governed by Reynolds equation and for an incompressible and isoviscous fluid with no-slip condition, the stationary Reynolds equation in the continuum range was given by

$$\nabla_T \cdot \left(\frac{-\rho h^3}{12\mu} \nabla_T p + \frac{\rho h}{2} (v_a + v_b) \right) - \rho \left((\nabla_T b \cdot v_b) - (\nabla_T a \cdot v_a) \right) = 0 \quad (1)$$

In this equation, ρ is density (kg/m^3), h is lubricant thickness (m), μ is viscosity (Pa.s), p is pressure (Pa), a is location (m) of the channel base, v_a is tangential velocity (m/s) of the chanl base, b is location (m) of the solid wall, and v_b represents the tangential velocity (m/s) of the solid wall. The rotating journal is considered to be a solid wall. Because the pressure is constant through the lubricant film thickness, COMSOL uses the tangential projection of the gradient operator, ∇_T, to calculate the pressure distribution on the lubricant surface. In this study, the term $\rho((\nabla_T b \ldots v_b) - (\nabla_T a \ldots v_a))$ equates to 0, so the governing equation simplifies to

$$\nabla_T \cdot \left(\frac{-\rho h^3}{12\mu} \nabla_T p + \frac{\rho h}{2} (v_a + v_b) \right) = 0 \quad (2)$$

2.2 Cavitation model

In hydrodynamic journal bearing system, journal rotates eccentrically with reference to bearing which develops a convergent and divergent region. In the convergent region, rotation of journal forces the lubricant into reduced area which results in an increase in lubricant pressure while results in negative pressure in the divergent zone. As the negative pressure starts to fall below atmospheric, the lubricant srts to cavitation in the divergent region. With the validated cavitation effect of Elrod and Adams [29] is considered and the flow in the journal bearing is divided in two regions:

- A full film region where the pressure varies but is limited from below by the cavitation pressure.
- A cavitation region where only part of the volume is occupied by the fluid. Because of the presence of the gas in the void fraction, the pressure in this region is assumed as constant and equal to the cavitation pressure.Elrod and Adams modified a general form of Reynolds equation by introducing a switch function, g, equal to 1 in the full fluid film zone (θ ≥ 1) and 0 in the cavitation zone (θ < 1). This switch function allows for solving single equation for the full film and the cavitation region and leads to a modified version of the average velocity used in the Reynolds equation:

$$V_{av} = V_{av,c} - gV_{av,p} \nabla_t p_f \quad (3)$$

where first and second term on right hand side correspond to the average Couette and average Poiseuille velocities, respectively. This switch function sets the average Poiseuille velocity is to zero in the cavitation region. Because the average Poiseuille velocity is set to zero in the cavitation region, the density needs to be a function of the pressure variable and it is defined as

$$\rho = \rho_c e^{\frac{p - p_c}{\beta}} \quad (4)$$

2.3 The bearing domain

The elastic deformation of bearing surface is due to pressure exerted by lubricant flow. The equilibrium equation governing the bearing domain is given below; [18];

$$\rho_b \ddot{d}_b = \nabla \cdot \sigma_b + F_b \tag{5}$$

where ρ_b represents density of bearing, $\ddot{d}_b$ shows local acceleration, σ_b is the stress tensor, F_b represents the body force vector and subscript b is used for bearing domain designation. The lubricant and bearing interact with each other and fluid pressure causes the bearing surface to deform which results in change in boundary condition. The nodes on the lubricant and bearing interface corresponds to the deformation compatibility and traction balancing;

$$d_f = d_b \tag{6}$$

$$n \cdot \tau_f = n \cdot \tau_b \tag{7}$$

where d_f and τ_f are the displacement as well as stress of lubricant field respectively, and d_b and τ_b are the bearing displacement as well as stress respectively.

In this investigation, fluid structure interaction problem is solved using dect computing method which is also known as the simultaneous solution approach [18]. In this lubricant and solid domain equations are initially linearized and then combined in the form of matrix;

$$\begin{bmatrix} A_{ff} & A_{fb} \\ A_{bf} & A_{bb} \end{bmatrix} \begin{bmatrix} \Delta X_f^k \\ \Delta X_b^k \end{bmatrix} = \begin{bmatrix} F_f \\ F_b \end{bmatrix} \tag{8}$$

where A_{ff}, A_{bb}, A_{fb} and A_{bf} are the matrix of system for lubricant, bearing and coupling effects correspondingly.F_f and F_b are the forces for the lubricant and bearing domain respectively. ΔX_f^k and ΔX_b^k are the solutions for the both domain whereas k is the iteration number.

The lubricant film thickness is the distance between the journal-fluid interface as well as the bearing-fluid interface, considering the elastic deformations between the two sliding surfaces. The thickness of fluid film for smooth surface $h_p(\theta)$ and for bearing with negative texturing Δh is given by Eqs. (9) and (10) respectively [18].

$$h_p = \mathrm{C}(1 + \varepsilon \cos\theta) + d_b \tag{9}$$

$$h = h_p + \Delta h + d_b \tag{10}$$

where h film thickness, C radial clearance, Δh groove height, d_b total elastic deformation of bearing surface.

2.4 Performance characteristics

The LCC of lubricant is calculated by taking integration of lubricant film pressure [11, 30].

$$F_f = \sqrt{\left(\int_0^H \int_0^{2\pi} Pr\cos\theta \, d\theta \, dz \int_0^H\right)^2 + \left(\int_0^H \int_0^{2\pi} Pr\sin\theta \, d\theta \, dz\right)^2} \tag{11}$$

The frictional force due to viscosity (*FF*) is calculated by [11, 30]

$$\mathrm{FF} = 2\pi \mathrm{R}^2 \mathrm{H} \mu \left(\frac{\mathrm{u}}{\mathrm{c}}\right) \tag{12}$$

where u is lubricant velocity and c is clearance between journal and bearing.

The coefficient of friction (*COF*) is derived by using ratio of friction force (FF) and LCC [21].

$$COF = \frac{FF}{F_f} \tag{13}$$

3 FSI model

The schematic diagram of a plain hydrodynamic journal bearing system is shown in Fig. 1a where Dj and Db are the journal diameter and inside bearing diameter. Journal center Oj and bearing center Ob is separated by eccentricity e and t is the bearing thickness as shown in Fig. 1a. The water lubricant flow is assumed to be constant with respect to time and other properties are assumed to be constant. The applied load (F) to journal is in vertical downward direction. Table 1 list the operating, geometrical and texturing parameters used for FSI analysis. Grooves are modeled in the region of 0–90°, 90–180° and 0°–180° along circumferential direction as shown in Fig. 1b–d. The axial spacing of 2 mm is kept in between adjacent grooves. Figure 1e shows enlarged view of groove shape texturing.

In the current study, three dimensional analysis of journal bearing was investigated using Fluid Structure Interaction (thin film flow and solid mechanics) physics of COMSOL Multiphysics. The finite element method is used for descretization of lubricant as well as bearing domain. The boundary conditions of the inside and outside surface of bearing were considered as fluid solid interface and fixed support respectively. The both ends of the bearing domain were imposed to zero deformation along with the axial direction. The boundary conditions of the inlet of lubricant and outlet of lubricant are respectively "pressure inlet" as well as "pressure outlet" with gauge pressure as zero Pa. The outer face of water lubricant was modeled as interface surface and inner surface was rotated with journal speed. Total 80,640 quadrilateral (mapped) elements and 185,660 prism shape elements were used for analysis of lubricant and plain bearing domain respectively as shown

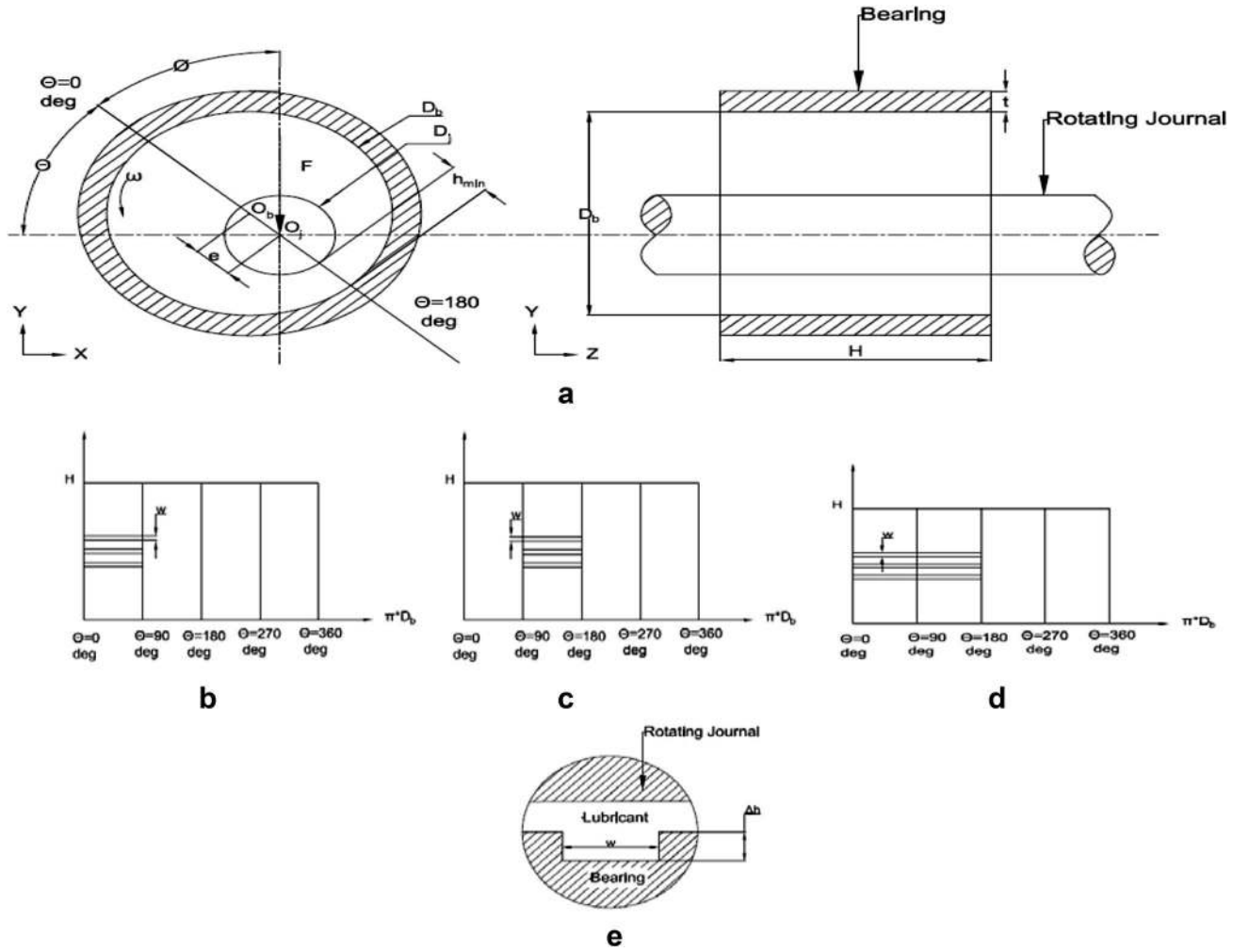

Fig. 1 Hydrodynamic journal bearing model with **a** Plain surface, **b** 0–90° groove region, **c** 90–180° groove region, **d** 0–180° groove region, **e** enlarged view groove region

Table 1 Input parameters for FSI analysis

Parameter	Value	Parameter	Value
Journal diameter (D_j)	80 (mm)	Groove numbers in Axial direction	1, **3**, 5
Bearing length (H)	80 (mm)	Groove width (w)	2 (mm)
Bearing thickness (t)	10 (mm)	Groove height (Δh)	20 (μm)
Eccentricity ratio (ε)	0.4, 0.5, **0.6**, 0.7	Circumferential groove region($\theta_1 - \theta_2$)	0–90, 90–180, 0–180
Radial clearance (C)	40 (μm)	Spacing between grooves (SP)	3 (mm)
Viscosity of water (μ)	0.001 (Pa s)	Elastic modulus of PTFE (E)	1400 (MPa)
Viscosity of water vapour (μ)	1.34E−5 (Pa s)	Density of PTFE (ρ_b)	2200 (kg/m^3)
Density of water (ρ)	998.2 (kg/m^3)	Poisson's ratio (η)	0.36
Density of water vapour	0.5542(kg/m^3)		
Journal speed [J_s] **1500**, 2000, 2500, 3000, 3500 [RPM]			

The bold values in table indicates reference values

The effect of number groove on perfromance analysis is carried out at that reference values

in Fig. 2a. The quality of meshing was checked and it was found 100% for lubricant domain. The minimum 94% element quality is observed at very less portion of bearing as shown in Fig. 2b.

The maximum and minimum size of element is 1.5 mm 0.004 mm respectively in case of lubricant domain whereas 1.75 mm and 0.004 mm in bearing domain. The mesh dependency investigation is carried out and fluid film pressure results are listed in Table 2. Further analysis of textured bearing system was carried out at maximum and minimum element size of 1 mm and 0.004 mm from case number 3.

4 Results and discussion

In this section validation of plain journal bearing, the influence of speed of journal and eccentricity ratio on lubricant pressure development, LCC, elastic deformation and COF is examined with different configurations [0–90°, 90–180°, 0–180°] of journal bearing system.

4.1 Validation

In this research work, first validation of FSI model is performed at rigid condition of bearing. Initially, investigation

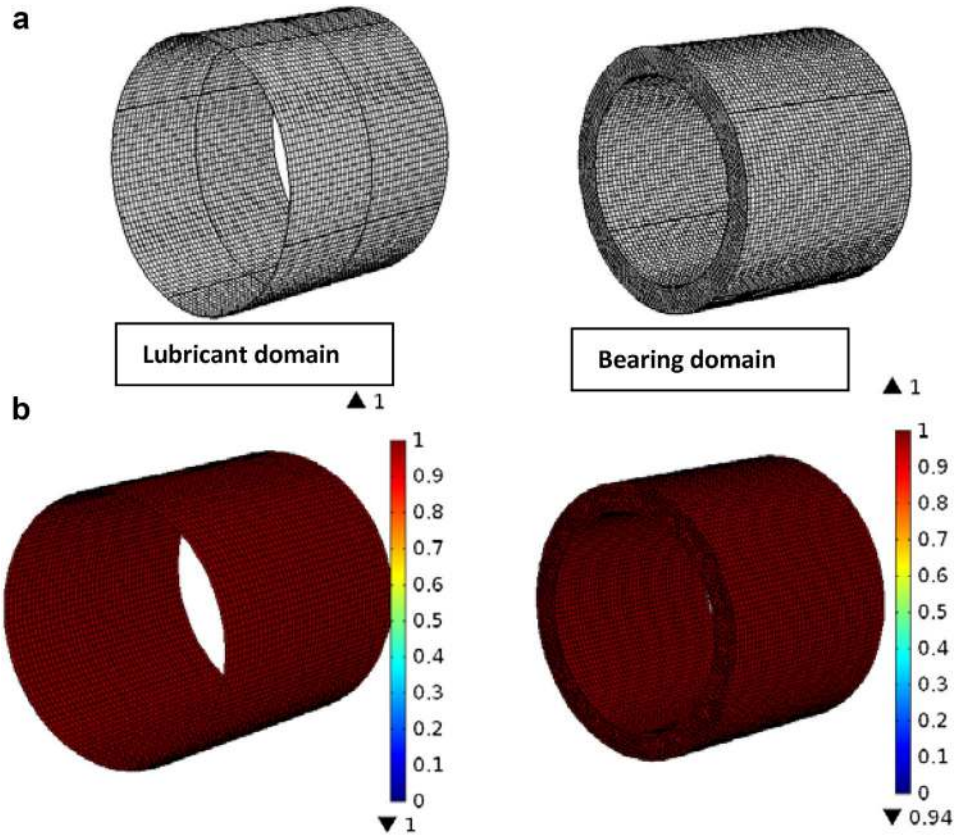

Fig. 2 Plain journal bearing with **a** Meshing of lubricant and bearing domain, **b** mesh quality

Table 2 Results for various sizes of mesh and precisions for 0–180 grooved bearing configuration

Case	1	2	3	4	5
Max. size of element in mm	2.25	2.00	1.75	1.5	1.25
Mini. size of element in mm	0.008	0.008	0.004	0.004	0.004
Total elements	346,387	477,932	697,863	1,106,881	1,937,185
Lubricant pressure in MPa	9.012	9.198	9.325	9.325	9.325

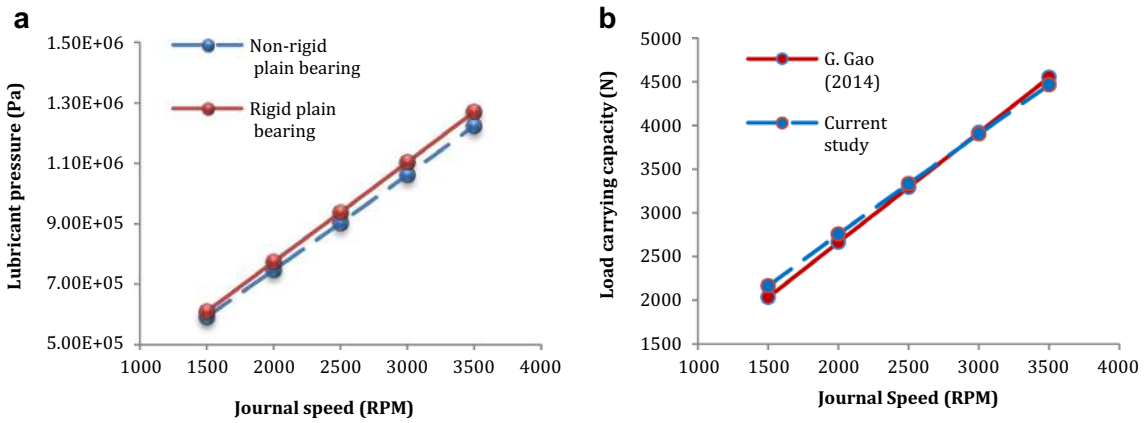

Fig. 3 Effect of journal speed on **a** lubricant film pressure and **b** LCC

is conducted for plain hydrodynamic journal bearing with rigid bearing and then considering the effect of deformation under different journal speeds. The simulation results are depicted in Fig. 3a. From Fig. 3a it is seen that development of fluid pressure in rigid bearing surface is more than non-rigid bearing surface. The LCC results are compared with experimental results presented in the literature [22- G. Gao] under the same input parameters as well as boundary conditions as shown in Fig. 3b. The results of LCC are calculated at different journal speed viz. 1500 RPM, 2000RPM, 2500RPM, 3000RPM and 3500RPM. These results shows very good agreement with error of 6.39%, 3.47%, 1.27%, 0.45% and 1.85% respectively.

4.2 Lubricant pressure field

The development of lubricant film pressure of water lubricated bearing with different configurations viz. 0°–90°, 90°–180° and 0°–180° grooved is carried out using FSI approach. Initially, investigation is conducted for plain hydrodynamic bearing with rigid bearing and then considering the effect of deformation on lubricant pressure. Figures 4 and 5 show the development of fluid pressure in plain and 0°–180° grooved journal bearing for various journal speeds viz, 1500 RPM, 2000RPM, 2500RPM, 3000RPM and 3500RPM. In Figs. 4 and 5 the dark brown colour shows maximum pressure zone whereas dark blue colour shows minimum pressure zone. Figures 4 and 5 also show the maximum displacement of bearing surface in cavitation region. From Fig. 4 it is observed that fluid pressure of 5.91150 MPa, 7.44653 MPa, 9.01680 MPa, 1.06183Mpa and 1.2226 MPa is developed respectively for various journal speeds. Further investigation is conducted for bearing with 0°–90°, 90°–180° and 0°–180° grooved regions under various journal speeds as well as for various eccentricity ratio.The mass fraction is equal to 1 in the full film region and less than 1 in the cavitation region where only part of the volume is occupied by the lubricant as shown in Figs. 6 and 7. These Figures shows maximum elastic deformation (micron) of bearing surface in cavitation region.

The influence of various journal speed on the development of lubricant pressure with 0°–90°, 90°–180° and 0°–180° grooved configurations. This investigation is carried out at eccentricity ratio of 0.6 and 3 number of groove. From Fig. 8a it was observed that as journal speed increased from 1500RPM to 3500RPM, development of lubricant film pressure increased linearly. The maximum lubricant film pressure was observed at journal speed of 3500RPM in case of 0°–180° grooved journal bearing configuration as compared with other configurations. At journal speed of 3500RPM, the maximum pressure 1.96 MPa, 1.90 MPa, 1.23 MPa and 1.22 MPa is developed in journal bearing with 0°–180° groove, 90°–180° groove, 0°–90° groove and plain surface. The maximum percentage enhancement in development of pressure is about 59.94% in 0°–180° grooved journal bearing system as compared with plain surface bearing. This is observed because development of lubricant film pressure is dependent on film thickness and bearing surface deformation. From the analysis it was observed that, maximum surface deformation is observed in plain journal bearing as compared with grooved bearings as shown in Figs. 4 and 5. The elastic deformation values (in micron unit) are shown in dark blue region (Cavitation region) as shown in Figs. 4 and 5. This deformation reduces the lubricant film pressure with increasing the lubricant film thickness.

Further, investigation was carried out at 1, 3 and 5 number of axial grooves with eccentricity ratio of 0.6 as depicted in Fig. 8b. From Fig. 8b it was seen that, as speed of journal increased, the development of lubricant pressure was increased linearly. The maximum pressure is observed for bearing with 5 grooves. It was also seen that, as number of grooves increased from 1 to 5, the value

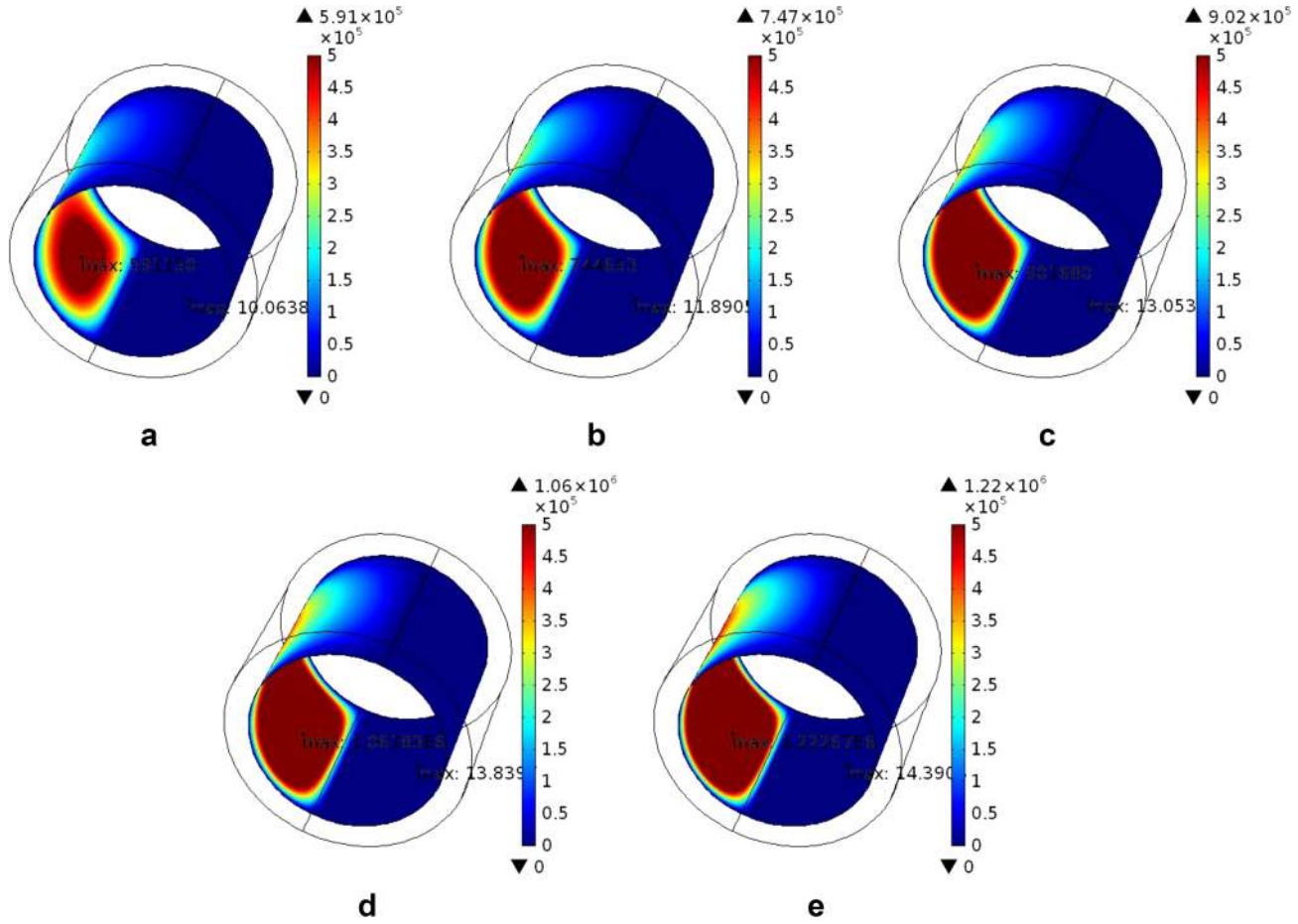

Fig. 4 Development of lubricant pressure in plain journal bearing at different journal speed **a** 1500RPM, **b** 2000RPM, **c** 2500RPM, **d** 3000RPM, and **e** 3500RPM at eccentricity ration of 0.6

of lubricant film pressure increased. At journal speed of 3500RPM, the maximum pressure value of 2.07 MPa, 1.96 MPa, 1.69 MPa and 1.22 MPa is observed in journal bearing with 5 grooves, 3 grooves, 1 groove and plain surface. The bearing surface with 5 grooves increased lubricant film pressure by 69.34% as compared with plain journal bearing.

Similarly, study was carried out to check effect of eccentricity ratio on the development of pressure in water lubricant. Figure 9a shows the development of lubricant film pressure at various eccentricity ratios viz. 0.4, 0.5, 0.6, and 0.7 for all the configurations. Same approach was implemented for journal bearing with 5 grooves, 3 grooves, 1 groove and plain surface as clearly shown in Fig. 9b. Figure 9a shows that as eccentricity ratio decreases from 0.7 to 0.4 the lubricant film pressure decreased non-linearly. The minimum lubricant film pressure was observed at eccentricity ratio of 0.4 whereas highest pressure is seen at eccentricity ratio of 0.7. At eccentricity ratio of 0.7, the highest pressure value of 1.15 MPa, 1.14 MPa, 0.889 MPa and 0.878 MPa was seen for bearing with 0°–180° grooved, 90°–180° grooved, 0°–90° grooved and plain surface respectively.

The effect of number of groove on the development of lubricant pressure at different eccentricity ratio was carried out at journal speed of 1500RPM. Bearing surface with 1 groove, 3 grooves and 5 grooves were considered for investigation. From Fig. 9b it was seen that maximum pressure was developed in case of bearing surface with 5 grooves as compared with other configurations. At eccentricity ratio of 0.7, the highest pressure value of 1.28 MPa, 1.15 MPa, 1.07 MPa and 0.889 MPa was seen in journal bearing with 5 grooves, 3 grooves, 1 groove and plain surface.

4.3 Load carrying capacity (LCC)

LCC is important performance characteristic of journal bearing and it was calculated by taking integration of lubricant film pressure. The influence of different journal speed and eccentricity ration on LCC was conducted with various grooved configurations of journal bearing.

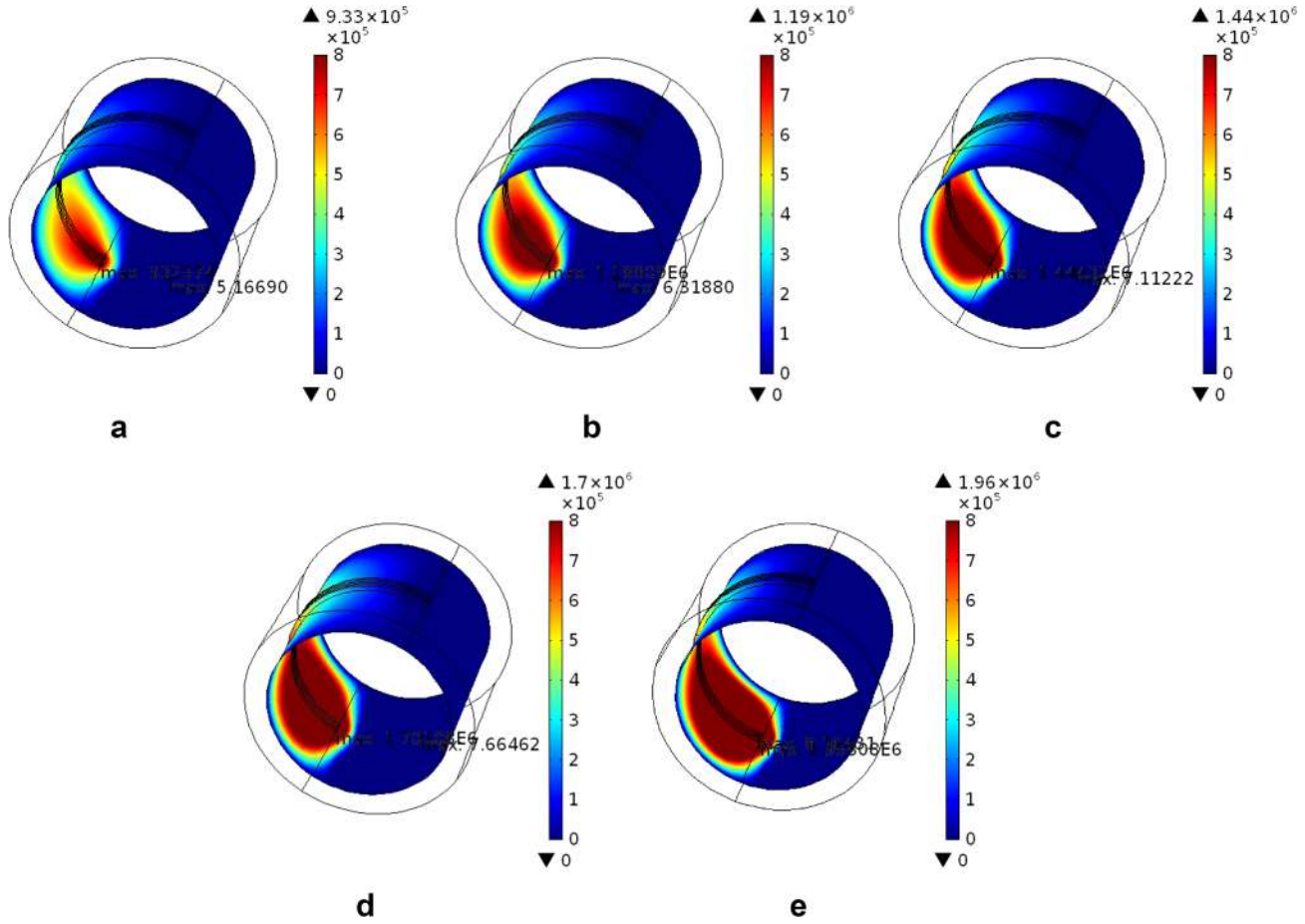

Fig. 5 Development of lubricant pressure in 0–180 deg grooved journal bearing at 3 grooves for different journal speed **a** 1500RPM, **b** 2000RPM, **c** 2500RPM, **d** 3000RPM, and **e** 3500RPM at eccentricity ratio of 0.6

First the influence of journal speed on LCC was studied with bearing configuration viz. 0°–90° grooved, 90°–180° grooved, 0°–180° grooved and plain journal bearing and their results are shown in Fig. 10a. Further investigation is conducted for bearing surface with 5 grooves, 3 grooves and 1 groove as depicted in Fig. 10b. From Fig. 10a it is clearly seen that, as journal speed increased, LCC in lubricant is increased. The maximum LCC is observed at journal speed of 3500 RPM for all the configurations of journal bearing system. At journal speed of 3500RPM, the maximum LCC of 6016.9 N, 5508.9 N, 4496.8 N and 4175.5 N is obtained for journal bearing with 0°–180° grooved, 90°–180° grooved, 0°–90° grooved and plain journal bearing respectively. At journal speed of 1500RPM, the maximum percentage improvement of 47.54 is observed in case of 0°–180° grooved journal bearing as compared with plain bearing system. This is observed because at journal speed of 1500RPM, elastic deformation of bearing surface is less as compared with other more journal speeds. Then analysis is carried out to examine the effect of number of grooves on the LCC under various journal speed as depicted in Fig. 10b. From Fig. 10b it is clearly seen that as number of groove increases, load carrying capacity increases. The maximum LCC of 7198.9 N 6016 N and 4924.1 N is observed at journal speed of 3500RPM for bearing with 5 grooves, 3 grooves and 1 groove. At journal speed of 1500RPM, the maximum improvement of 76.29% in LCC is observed in case of bearing with 5 grooves as compared with plain journal bearing system.

The influence of an eccentricity ratio on LCC of different configurations of bearing is shown in Fig. 11a. From Fig. 11a it is seen that as an eccentricity ratio is decreased from 0.7 to 0.4, LCC is decreased non-linearly. The minimum LCC is observed at eccentricity ratio of 0.4 in all configurations. It is also observed that maximum LCC of 3633.6 N is seen in 0°–180° grooved journal bearing at eccentricity ratio of 0.7. But maximum improvement in LCC of 74.30% is observed at eccentricity ratio of 0.4. Further investigation is carried out under different number of grooves and their results are shown in Fig. 11b. From Fig. 11b it is seen that minimum LCC is observed

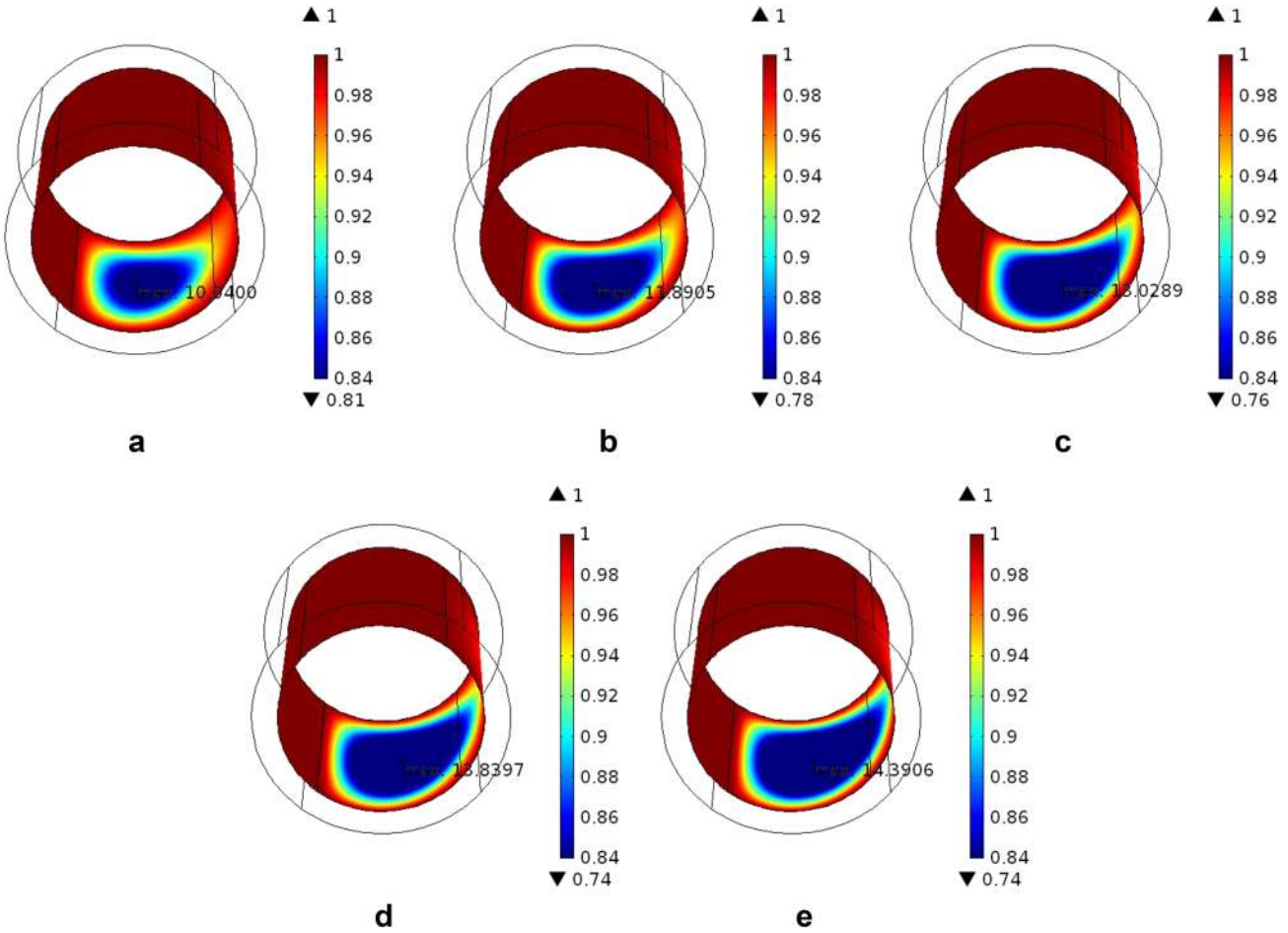

Fig. 6 The lubricant mass fractionin plain journal bearing at different journal speed **a** 1500RPM, **b** 2000RPM, **c** 2500RPM, **d** 3000RPM, and **e** 3500RPM at eccentricity ration of 0.6

in bearing with 1 groove as compared along with bearing with 5 grooves and 3 grooves. At eccentricity ratio of 0.7, the maximum LCC of 4217 N, 3633 N and 3110 N is seen in bearing with 5 grooves, 3 grooves and 1 groove.

4.4 Effect on coefficient of friction

COF is an important performance characteristic factor of journal bearing system. The effect of various groove location and number of groove on the COF is studied under various journal speed viz. 1500RPM, 2000RPM, 2500RPM, 3000RPM and 3500RPM and its results are plotted in Fig. 12a, b. From Fig. 12a it is seen that as speed of journal increases, COF increases non-linearly. The minimum COF is observed in 0°–180° grooved journal bearing as compared with other configurations. The minimum value of COF is observed at journal speed of 1500RPM for all the configurations. At a journal speed of 1500RPM, the minimum COF of 0.000780, 0.000866, 0.000883 and 0.000957 is observed for journal bearing with 0°–180° grooved, 90°–180° grooved, 0°–90° grooved and plain surface. The maximum 23% reduction of COF is achieved in case of 0°–180° grooved journal bearing as compared with plain journal bearing system. Further analysis is carried out for 0°–180° grooved journal bearing with number of grooves. The influence of number of grooves on the COF is shown in Fig. 12b. It is observed that, journal bearing with 5 grooves shows minimum COF as compared with other configurations. It is also observed that at journal speed of 3500RPM, maximum 49.20% reduction of COF is achieved as compared with plain journal bearing system.

Similarly the influence of eccentricity ratio on COF is examined for bearing with various groove location and number of groove as shown in Fig. 13a, b respectively at journal speed of 1500RPM. From Fig. 13a it is clearly seen that as an eccentricity ratio value increases from 0.4 to 0.7, COF decreases non-linearly. At eccentricity ratio of 0.4, the minimum of COF is observed for all the configurations. The minimum COF of 0.000780, 0.000886, 0.000862 and 0.000957 is seen in journal bearing with

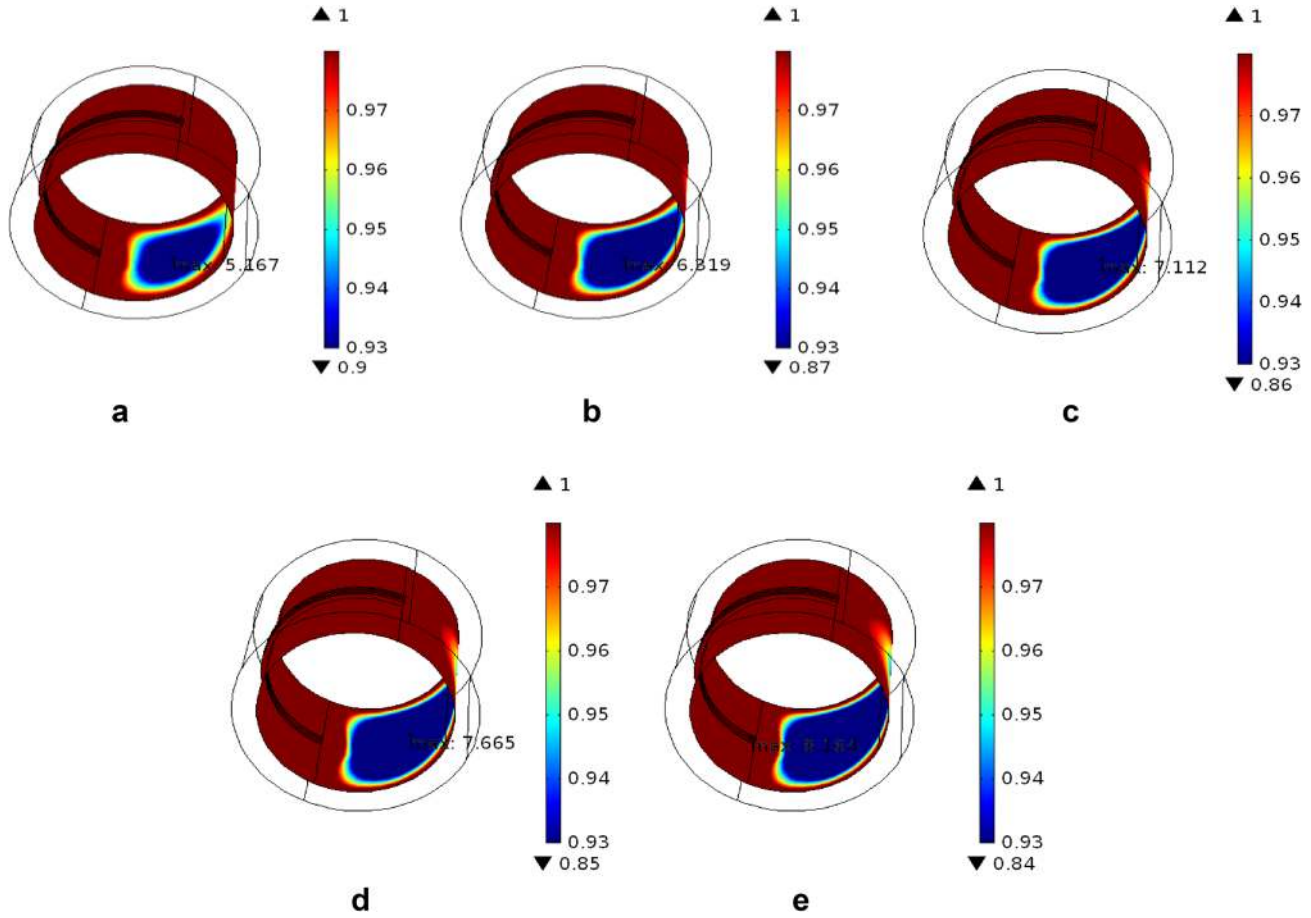

Fig. 7 The lubricant mass fractionin plain journal bearing at 3 grooves fordifferent journal speed **a** 1500RPM, **b** 2000RPM, **c** 2500RPM, **d** 3000RPM, and **e** 3500RPM at eccentricity ration of 0.6

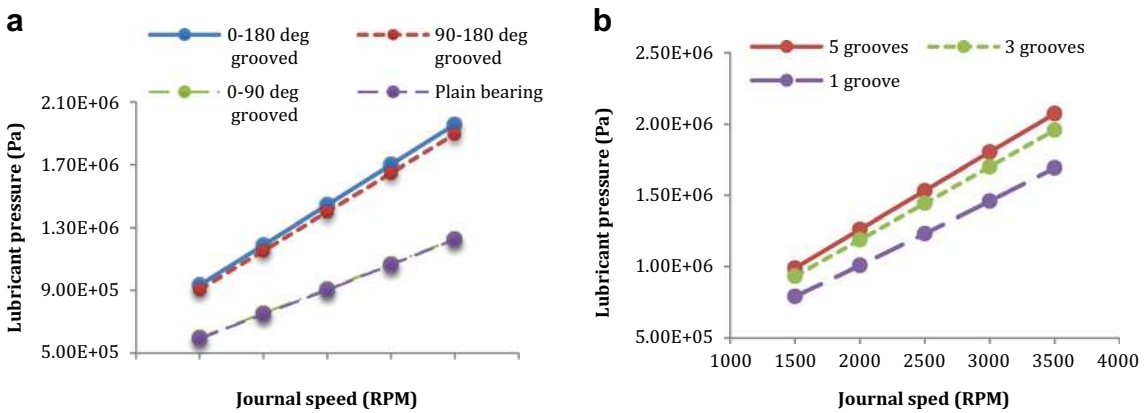

Fig. 8 Effect of journal speed on lubricant pressure with **a** different grooved location and **b** number of axial groove

0°–180° grooved, 90°–180° grooved, 0°–90° grooved and plain surface. Then investigation is carried out for 0°–180° grooved journal bearing configuration to study the influence of number of grooves on COF. As shown in Fig. 13b, as number of groove increases, COF between sliding surfaces decreases. The minimum COF is obtained

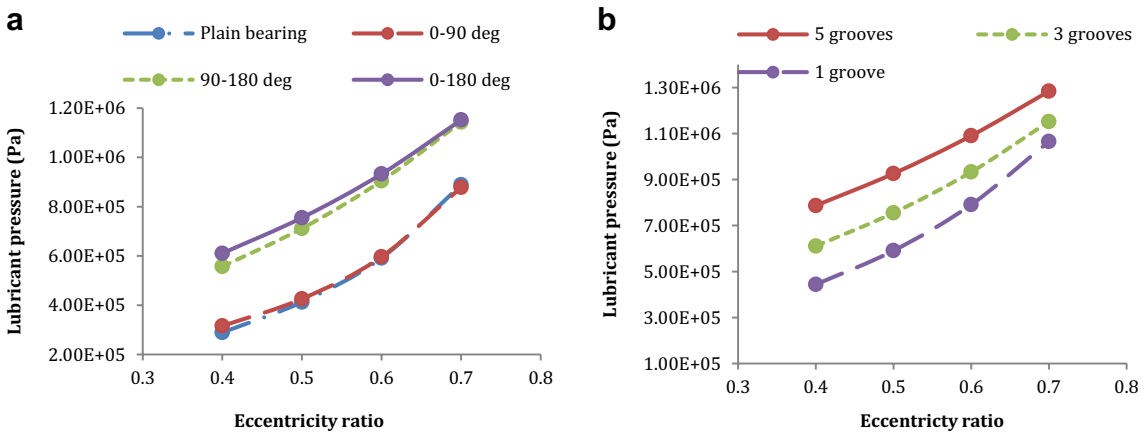

Fig. 9 Effect of eccentricity ratio on lubricant pressure with **a** different grooved location and **b** number of axial groove

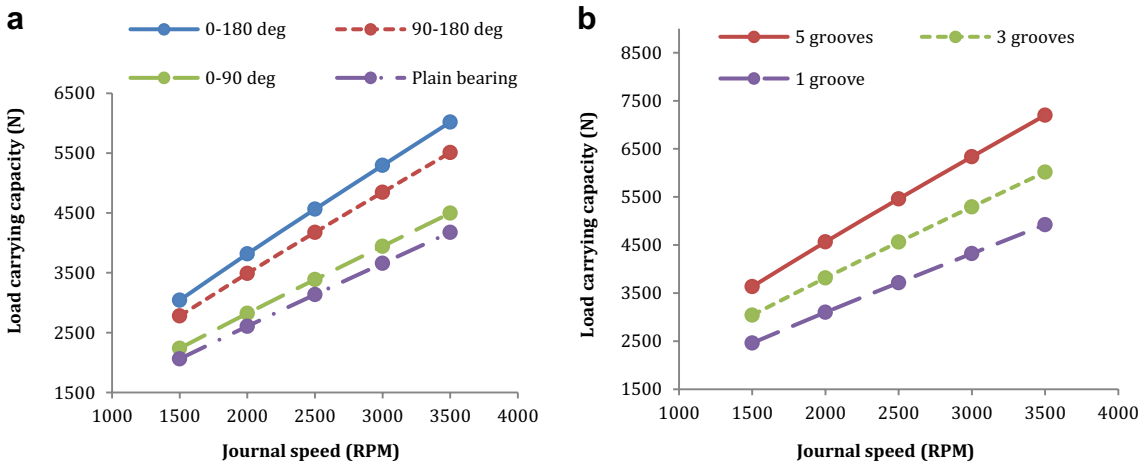

Fig. 10 Effect of journal speed on LCC with **a** different grooved location and **b** number of axial groove

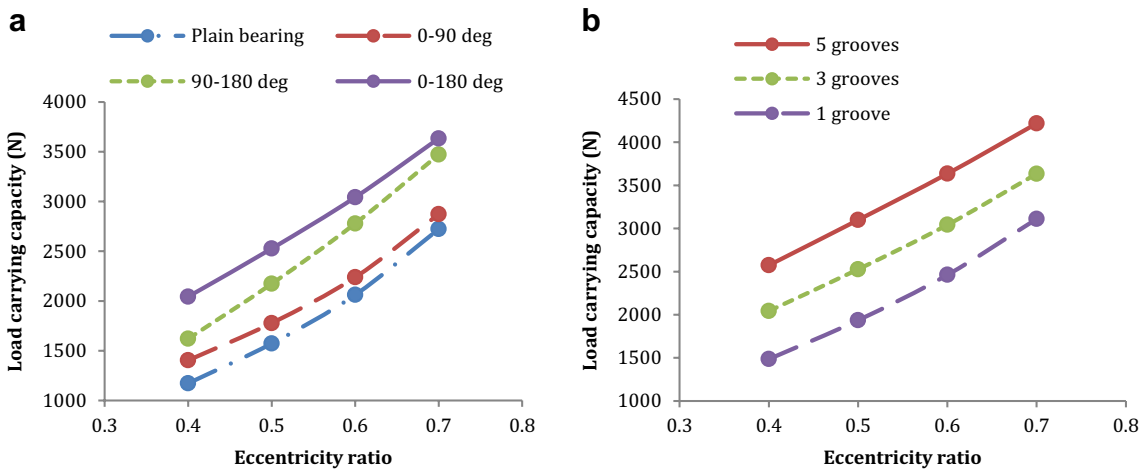

Fig. 11 Effect of eccentricity ratio on LCC with **a** different grooved location and **b** number of axial groove

in case of journal bearing with 5 grooves. The maximum 49.81% reduction of COF is achieved for 0°–180° grooved journal bearing with 5 number of grooves.

4.5 Effect on elastic deformation

Elastic deformation of solid domain is due to development of lubricant film pressure in journal bearing system.

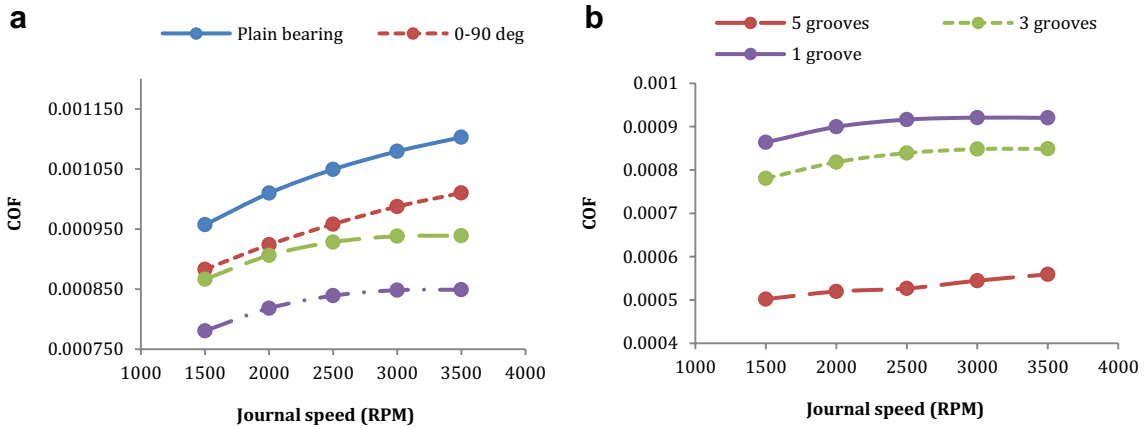

Fig. 12 Effect of journal speed on COF with **a** different grooved location and **b** number of axial groove

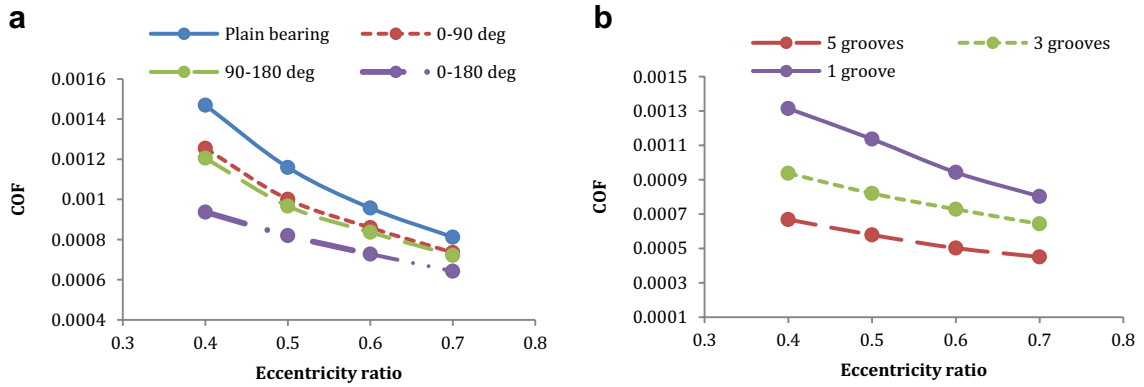

Fig. 13 Effect of eccentricity ratio on COF with **a** different grooved location and **b** number of axial groove

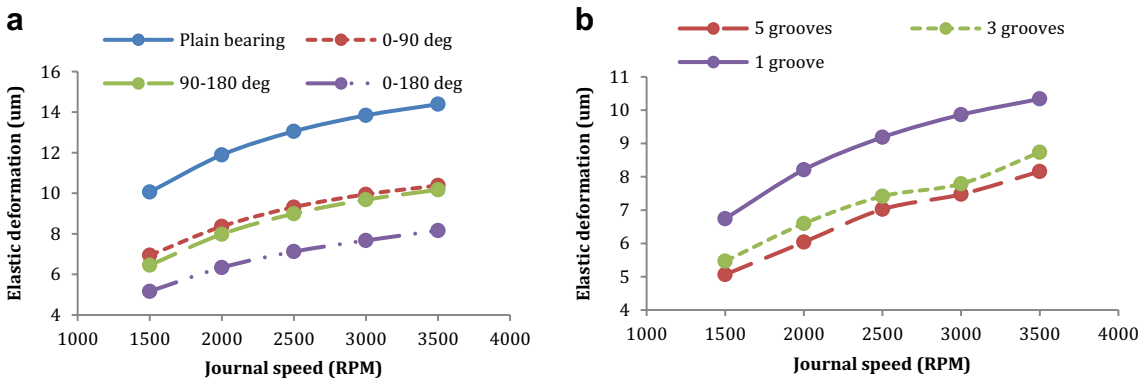

Fig. 14 Effect of journal speed on elastic deformation with **a** different grooved location and **b** number of axial groove

It depends on various operating parameters viz. external load, journal speed, clearance, bearing material properties etc. In this paper, PTFE material of Young's Modulus of 210 MPa and Poisson's ratio of 0.36 is considered. Lubricant Structure Interaction method is used to examine elastic deformation under various journal speeds. Figure 14 shows the influence of journal speed on elastic deformation for all configurations. From Fig. 14a it is seen that as journal speed increases from 1500RPM to 3500RPM, elastic deformation of bearing surface increases. The maximum deformation is observed at journal speed of 3500RPM for all the configurations. It is also seen that maximum elastic deformation is observed in plain journal bearing system whereas minimum deformation is observed in 0°–180° grooved journal bearing. These deformation values for plain and 0°–180° grooved journal bearing systems are shown in dark blue colour region after brown colour in Figs. 4 and 5 respectively. At journal speed of 3500RPM, the elastic deformation of 8.15 µm, 10.17 µm, 10.38 µm and 14.39 µm is observed for journal bearing with 0°–180° grooved, 90°–180° grooved, 0°–90° grooved and plain surface. This elastic deformation decreases the lubricant film pressure. Further analysis is carried out to examine the effect of number of grooves on the elastic deformation of bearing surface. This investigation is carried out for 0°–180° grooved bearing under various journal speed as clearly shown in Fig. 14b. From Fig. 14b it is observed that as number of groove increases, elastic deformation decreases. The maximum elastic deformation of 10.33 µm, 8.93 µm and 8.15 µm is observed for journal bearing with 1 groove, 3 grooves and 5 grooves respectively. This developed elastic deformation significantly affects the bearing performance characteristics.

5 Conclusions

In this study, investigation of water lubricated surface textured bearing with various configurations is carried out under various journal speed and eccentricity ratio using Fluid Structure Interaction method. In the investigation, different performance characteristic factors viz. lubricant pressure, LCC and COF are examined. Initially, the influence of groove location on the performance of bearing is examined for selection of best configuration and then effect of number of groove on performance is examined for selected configuration. Based on FSI based analysis following conclusions is summarized.

1. From FSI analysis of non rigid bearing surface, it is observed that, elastic deformation significantly affects the bearing performance characteristics. It reduces the lubricant film pressure, LCC and COF.
2. From the analysis, it is observed that 0°–180° grooved journal bearing with 5 grooves shows maximum lubricant pressure, LCC, and low COF as compared with other configurations.
3. It is also seen that, highest elastic deformation is seen in plain journal bearing system in cavitation region as compared with other configurations.
4. A 0°–180° grooved journal bearing with 5 grooves shows 69.34%, 72.41%, and 49.30% improved performance in lubricant pressure, LCC and COF at journal speed of 3500RPM and eccentricity ratio of 0.6.

Compliance with ethical standards

Conflict of interest On behalf of all authors, the corresponding author states that there is no conflict of interest.

References

1. Wang X, Koji K, Koshi A, Kohj A (2003) Loads carrying capacity map for the surface texture design of SiC thrust bearing sliding in water. Tribol Int 36:189–197
2. Brizmer V, Kligerman Y, Etsion I (2003) A laser surface textured parallel thrust bearing. Tribol Trans 46:397–403
3. Wang Y-Q, Li C (2011) Numerical analysis of hydrodynamic lubrication on water-lubricated rubber bearings. Adv Mater Res 299–300:12–16
4. Wang J, Yan F, Xue Q (2009) Tribological behavior of PTFE sliding against steel in sea water. Wear 267:1634–1641
5. Su B, Huang L, Huang W, Wang X (2018) Observation on the deformation of dimpled surface in soft-EHL contacts. Tribol Int 119:521–530
6. Habchi W, Eyheramendy D, Vergne P, Morales-Espejel G (2008) A full system approach of the elastohydrodynamic line/point contact problem. J Tribol 130:021501.1–021501.10
7. Gertzos K, Nikolakopoulos P, Papadopoulos C (2008) CFD analysis of journal bearing hydrodynamic lubrication by Bingham lubricant. Tribol Int 41:1190–1204
8. Hartinger M, Dumont ML, Ioannides S, Gosman D, Spikes H (2008) CFD modeling of a thermal and shear thinning elastohydrodynamic line contact. J Tribol 130:041503.1–041503.16
9. Shenoy SB, Pai R, Rao D, Pai RB (2009) Elasto-hydrodynamic lubrication analysis of full 360 journal bearing using CFD and FSI techniques. World J Model Simul 5:315–320
10. Liu H, Xu H, Ellison PJ, Jin Z (2010) Application of computational lubricant dynamics and fluid–structure interaction method to the lubrication study of a rotor–bearing system. Tribol Lett 38:325–336
11. Shinde A, Pawar P (2017) Effect of partial grooving on the performance of hydrodynamic journal bearing. Ind Lubr Tribol 69(4):574–584
12. Shinde A, Pawar P, Shaikh P, Wangikar S, Salunkhe S, Dhamgaye V (2018) Experimental and numerical analysis of conical shape

hydrodynamic journal bearing with partial texturing. Procedia Manuf 20:300–310
13. Shinde A, Pawar P, Gaikwad S, Shaikh P, Khedkar Y (2018) Analysis of water lubricated bearing with different features to improve the performance: green tribology. Springer International Publishing AG, Cham
14. Shinde A, Pawar P, Gaikwad S, Kapurkar R, Parkhe A (2018) Numerical analysis of deterministic micro-textures on the performance of hydrodynamic journal bearing. Mater Today Proc Part 1 5(2):5999–6008
15. Gao G, Yin Z, Jiang D, Zhang X (2014) Numerical analysis of plain journal bearing under hydrodynamic lubrication by water. Tribol Int 75:31–38
16. Shi L, Wang X, Su X, Huang W, Wang X (2016) Comparison of the Load-carrying performance of mechanical gas seals textured with microgrooves and microdimples. J Tribol 138:021701
17. Bouyer J, Fillon M (2004) On the significance of thermal and deformationeffects on a plain journal bearing subjected to severe operating conditions. J Tribol 126(4):819–822
18. Lin Q, Bao Q, Li K, Khonsari MM, Zhao H (2018) An investigation into the transient behavior of journal bearing with surface texture based on fluid-structure interaction approach. Tribol Int 118:246–255
19. Profito FJ, Zachariadis DC (2015) Partitioned fluid-structure methods applied to the solution of elastohydrodynamic conformal contacts. Tribol Int 81:321–332
20. Hili MA, Bouaziz S, Maatar M, Fakhfakh T, Haddar M (2010) Hydrodynamic and elastohydrodynamic studies of a cylindrical journal bearing. J Hydrodyn 22(2):155–163
21. Meng FM, Zhang L, Liu Y, Li TT (2015) Effect of compound dimple on tribological performances of journal bearing. Tribol Int 91:99–110
22. Tala-Ighil N, Fillon M (2015) Surface texturing effect comparative analysis in the hydrodynamic journal bearings. Mech Ind 16:302
23. Jadhav S, Thakre GD, Sharma SC (2019) Influence of MHD lubrication and textured surface in EHL line contact. Front Mech Eng 5:33. https://doi.org/10.3389/fmech.2019.00033
24. Tauviqirrahman M, Pratama A, Jamari Muchamad (2019) Hydrodynamic lubrication of textured journal bearing considering slippage: two dimensional CFD analysis using multiphase cavitation model. Tribol Ind 41(3):401–415
25. Tala-Ighil N, Maspeyrot P, Fillon M, Bounif A (2007) Effects of surface texture on journal-bearing characteristics under steady-state operating conditions. Proc Inst Mech Eng Part J J Eng Tribol 221:623–633
26. Gu C, Meng X, Xie Y, Yang Y (2016) Effects of surface texturing on ring/liner friction under starved lubrication. Tribol Int 94:591–605
27. Cupillard S, Glavatskih S, Cervantes MJ (2008) Computational fluid dynamics analysis of a journal bearing with surface texturing. Proc Inst Mech Eng Part J J Eng Tribol 222(2):97–108
28. Yu R, Chen W, Li p (2016) The analysis of elastohydrodynamic lubrication in the textured journal bearing. Proc Inst Mech Eng Part J J Eng Tribol 230(10):1197–1208
29. Elrod HG, Adams ML (1974) A computer program for cavitation and starvation problems, leeds-lyon conference on cavitation. Leeds University. England (Available from BHRA, Cranfield, England)
30. Shinde AB, Pawar PM, Ronge BP, Bhuse PK, Parkhe AK, Jadhav PV (2020) Optimization of multiple performance characteristics of surface micro-textured journal bearing. In: Pawar P, Ronge B, Balasubramaniam R, Vibhute A, Apte S (eds) Techno-Societal 2018. Springer, Cham, pp 377–389